

Coherent control of atomic spin currents in a double well

H. T. Ng¹ and Shih-I Chu^{1,2}

¹*Center for Quantum Science and Engineering, Department of Physics,
National Taiwan University, Taipei 10617, Taiwan and*

²*Department of Chemistry, University of Kansas, Lawrence, Kansas 66045, USA*

(Dated: August 6, 2018)

We propose a method for controlling the atomic currents of a two-component Bose-Einstein condensate in a double well by applying an external field to the atoms in one of the potential wells. We study the ground-state properties of the system and show that the directions of spin currents and net-particle tunneling can be manipulated by adiabatically varying the coupling strength between the atoms and the field. This system can be used for studying spin and tunneling phenomena across a wide range of interaction parameters. In addition, spin-squeezed states can be generated. It is useful for quantum information processing and quantum metrology.

PACS numbers: 03.75.Lm, 03.75.Mn, 05.60.Gg

I. INTRODUCTION

Spin and tunneling phenomena are of fundamental interests in understanding quantum behaviors of particles. They are also important in the applications using solid-state devices such as sensors and data storage [1]. In addition, manipulation of the quantum state of a single spin is essential in implementing quantum information processing [2].

Recently, the tunneling dynamics of ultracold atoms has been observed in a double well [3] and optical lattices [4], where the experimental parameters can be widely tuned. Moreover, high-fidelity single-spin detection of an atom has been realized in an optical lattice [5, 6] and atom-chip [7], respectively. Such sophisticated techniques of manipulating ultracold atoms open up the possibilities for the study of intriguing quantum phenomena never possible before.

In this paper, we propose a method to control the tunneling dynamics of a two-component Bose-Einstein condensate (BEC) in a double well [8] by applying an external field to the atoms in one of the potential wells. In fact, the methods for controlling of tunneling in a double-well BEC have been suggested by driving the double-well potentials [9] and by applying a symmetry-breaking field [10], respectively. Besides, a number of methods for manipulating the atomic motions in an optical lattice have been proposed such as using external fields for vibrational transitions between adjacent sites [11], tilting the lattice potential [12] and periodic modulation of the lattice parameters [13].

Here we show that the spin and tunneling dynamics of atoms can be manipulated by adiabatically changing the coupling strength of the field. This approach can be used for studying the spin and tunneling related phenomena in a controllable manner. For example, the directions of “spin currents” such as *parallel*- and *counter*-flows can be controlled by appropriately adjusting the interaction parameters. Here the “spin currents” refer to the two atomic currents of a condensate of ⁸⁷Rb atoms with the two different hyperfine levels [14]. Apart from changing

the internal states of atoms, the external field gives rise to *net-particle tunneling*. It is different to the situation of co-tunneling of the two component condensates in a double well [8, 15] in which the number difference of atoms between the wells is equal during the tunneling process.

In addition, the tunnel behaviors are totally different in the limits of weak and strong atomic interactions. In the regime of weak atomic interactions, the atoms smoothly tunnel through the other well. On the contrary, the discrete steps of tunneling are shown in the limit of strong atomic interactions. The coherent control of single-atom tunneling can thus be achieved. This method can be utilized for atomic transport.

Furthermore, we investigate the production of spin squeezing [16, 17] in this system. The occurrence of spin-squeezing can indicate multi-particle entanglement [18]. We show that spin-squeezed states can be dynamically generated by slowly changing the coupling strength of the field. This can be used for preparing entangled states and quantum metrology [19].

This paper is organized as follows: In Sec. II, we introduce the system of a two-component BEC in a double well, where the atoms in the left potential well are coupled to the laser field. In Sec. III, we study the ground-state properties of the system. In Sec. IV, we propose a method to adiabatically transfer the atoms to the other well. In Sec. V, we investigate the generation of multi-particle entanglement using this method. We provide a summary in Sec. VI. In the Appendix, we derive an effective Hamiltonian describing the coupling between the two internal states with the lasers.

II. SYSTEM

We consider a condensate of ⁸⁷Rb atoms with two hyperfine levels $|e\rangle = |F = 2, m_F = 1\rangle$ and $|g\rangle = |F = 1, m_F = -1\rangle$ of the $5S_{1/2}$ ground state [14] confined in a symmetric double-well potential [8]. An external field is applied to the atoms in one of the potential wells. The schematic of the system is shown in Fig. 1(a).

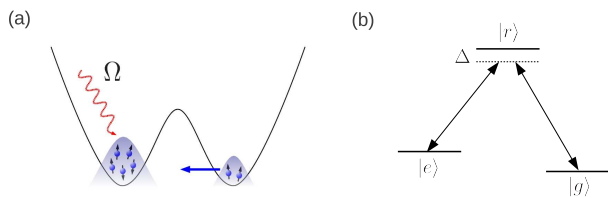


FIG. 1. (Color online) (a) Schematic of a two-component Bose-Einstein condensate in a double well. An external field is applied to the atoms in the left potential well. (b) Energy levels for the atoms. The two internal states $|e\rangle$ and $|g\rangle$ are coupled via the upper state $|r\rangle$.

This system can be described by the total Hamiltonian $H_{\text{tot}} = H_0 + H_1$, where H_0 and H_1 are the Hamiltonians describing the external and internal degrees of atoms.

We adopt the two-mode approximation to describe the atoms in deep potential wells [8]. Since the scattering lengths of the different hyperfine states of ^{87}Rb are very similar [20], we assume that the intra- and inter-component interactions are nearly the same. The Hamiltonian H_0 can be written as ($\hbar = 1$)

$$H_0 = -J(e_L^\dagger e_R + e_R^\dagger e_L + g_L^\dagger g_R + g_R^\dagger g_L) + U[(n_{eL} + n_{gL})^2 + (n_{eR} + n_{gR})^2], \quad (1)$$

where $\alpha_L(\alpha_R)$ and $n_{\alpha L}(n_{\alpha R})$ are annihilation operator of an atom and number operator in the left(right) potential well, for $\alpha = e, g$. The total number N of atoms is conserved in this system. To ensure the validity of two-mode approximation, we assume that the trapping energy is much larger than the atomic interaction energy [9, 21], i.e., $\omega_0 \gg UN$, where ω_0 is the effective trapping frequency of the potential well.

We can make a rough estimation of the experimental parameters within the two-mode approximation. For ^{87}Rb , the scattering length a is about 5 nm. We take the frequencies ω_y and ω_z of the transverse trapping potentials to be about $2\pi \times 1$ kHz. Indeed, the barrier height and the separation between the two potential minima can be varied [22] by appropriately splitting the potential. We consider that the barrier height V_b can be tuned [22] from $2\pi \times 50$ to $2\pi \times 250$ Hz and the separation $2x_0$ between two wells are 2 and 4 μm . The effective frequency $\omega_0 = \sqrt{8V_b/(m x_0^2)}$ [21] is related to the barrier height V_b and the separation $2x_0$. This gives the effective frequency ω_0 ranging from $2\pi \times 220$ to $2\pi \times 350$ Hz, and the interaction strength U ranges between $2\pi \times 2.7$ and $2\pi \times 3.4$ Hz. From these estimations, the number N of atoms must be less than 100 to maintain the validity of two-mode approximation [9, 21]. We also estimate the ratio U/J of the atomic strength and tunneling strength which ranges from 0.05 to 300.

Without loss of generality, we consider an external field to be applied to the atoms in the left potential well. The two internal states can be coupled via the upper transition of the D_2 line of ^{87}Rb [23] by using the two laser

beams with different circular polarizations as shown in Fig. 1(b). This upper state $|r\rangle$ can be adiabatically eliminated due to the large detuning. In the Appendix A, we derive an effective Hamiltonian for describing the interaction between the two internal states and the lasers. In the interaction picture, the Hamiltonian H_1 is given by [24]

$$H_1 = \Delta(n_{eL} + n_{eR}) + \hbar\Omega(e_L^\dagger g_L + \text{H.c.}), \quad (2)$$

where Δ is the detuning between the atomic transition ($|r\rangle$ and $|e\rangle$) and the laser field, and Ω is the effective coupling strength between the atoms and external field. A tightly focused laser can be applied to the atoms in one of the potential well. In fact, a tightly focused laser has been used for addressing a single atom in an optical lattice [6], where the full-width at half-maximum (FWHM) of the diameter of laser beam is within 1 μm [6]. The separation between the two potential wells is about several μm in the experiment [3]. Therefore, the effects of the external lasers on the atoms in the other well are small.

III. GROUND-STATE PROPERTIES OF THE COUPLED ATOM-LASER SYSTEM

Now we study how the ground state properties of the BEC affected by the local external field. In Fig. 2, we plot the population differences ($\langle n_{\alpha L} \rangle - \langle n_{\alpha R} \rangle$) versus the coupling strengths Ω for the atoms in the two different internal states $|\alpha\rangle$ and $\alpha = e, g$. For the cases of even number N of atoms, there is an equal number of atoms in the two wells in the absence of the external field, i.e., $\Omega = 0$. The external field causes the energy bias between the two wells. Thus, the population difference becomes larger when the coupling strength increases.

Moreover, the system exhibits totally different behaviors in the regimes of weak and strong atomic interactions. For weak atomic interactions, the population differences smoothly vary as a function of the coupling strength as shown in Figs. 2(a) and (c). Also, a larger number of atoms are in the state $|g\rangle$ due to the larger detuning Δ .

In Figs. 2(b) and (d), we plot the population differences versus the coupling strengths Ω in the regime of strong atomic interactions. We can see that discrete steps of the population difference for atoms in the state $|g\rangle$ are shown when the coupling strength increases. However, the discrete feature is not obvious for the atoms in the state $|e\rangle$. In Fig. 2(b), the atoms, in the two different internal states, distribute in the opposite potential wells for small Ω . When Ω becomes larger, both component of atoms populate in the left potential well. This result shows that the population difference of atoms in the two internal states depends on the coupling strength and also the detuning between the atoms and field.

To proceed, we investigate the relationship between the total population difference of atoms ($\langle n_{eL} + n_{gL} - n_{eR} - n_{gR} \rangle$) and the coupling strength Ω . In Fig. 3, we

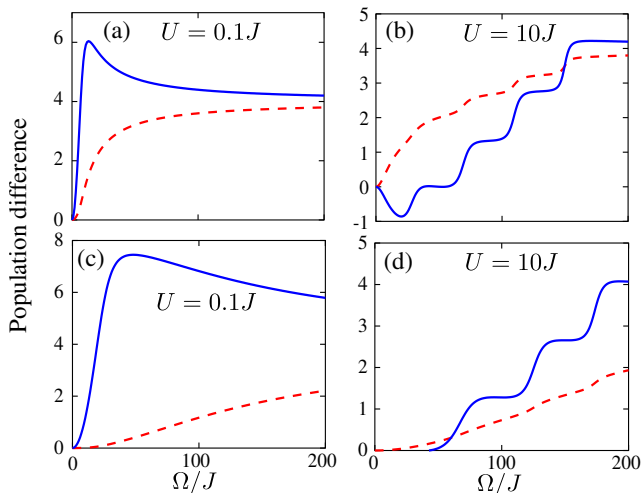


FIG. 2. (Color online) Population differences are plotted as a function of Ω/J for the ground state of the system and $N = 8$. The parameters are shown: (a) and (b) $\Delta = 20J$; (c) and (d) $\Delta = 200J$. The ground state $|g\rangle$ and excited state $|e\rangle$ of atoms are denoted by blue-solid and red-dotted lines, respectively.

plot the total population differences as a function of the coupling strength Ω for different strengths U of atomic interactions. The external field leads to the population imbalance between two wells in both regimes of weak and strong atomic interactions. For weak atomic interactions, the population difference smoothly increases with Ω . When the atomic interactions become strong, the discrete steps of population differences are shown in Fig. 3. The sharper discrete steps are shown for larger U . In this case, a single atom is only allowed to tunnel through the other well for the specific coupling strengths.

A. Tunneling condition in the limit of strong atomic interactions

We now discuss the tunneling condition in the limit of strong atomic interactions. Since the tunnel couplings are negligible in this regime, the numbers of atoms in the two wells are conserved. We assume that there are $N/2 + n$ and $N/2 - n$ atoms in the left and right wells. For convenience, we define the angular momentum operators: $S_{jx} = (g_j e_j^\dagger + e_j g_j^\dagger)/2$, $S_{jy} = (g_j e_j^\dagger - e_j g_j^\dagger)/2i$ and $S_{jz} = (e_j^\dagger e_j - g_j^\dagger g_j)/2$, and $j = L, R$. To diagonalize the Hamiltonian H_{tot} , we apply the transformation as

$$S_{Lx} = \cos\theta S'_{Lx} - \sin\theta S'_{Lz}, \quad (3)$$

$$S_{Lz} = \cos\theta S'_{Lz} + \sin\theta S'_{Lx}. \quad (4)$$

By setting the term, $\Delta \sin\theta + 2\Omega \cos\theta$, to zero, the total Hamiltonian can be diagonalized as

$$H'_{\text{tot}} = \Delta S_{Rz} + \hbar \sqrt{\Delta^2 + 4\Omega^2} S'_{Lz} + U(N^2/2 + 2n^2) + \hbar \Delta N/2, \quad (5)$$

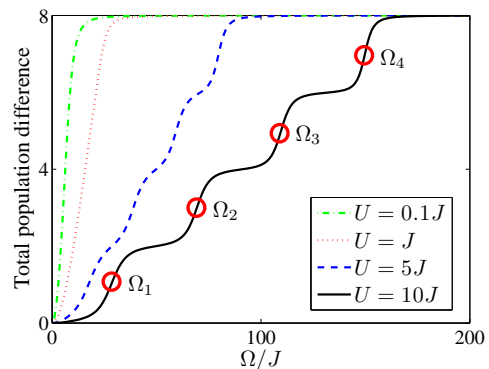


FIG. 3. (Color online) Plot of the total population difference versus Ω/J for the ground state with the different strengths U of atomic interactions. The parameters are used: $N = 8$ and $\Delta = 20J$. The values of Ω_n in Eq. (6) are marked with the red empty circles.

and its ground-state energy E_n^G is given by

$$E_n^G = -\Delta(N/2 - n)/2 - \sqrt{\Delta^2 + 4\Omega^2(N/2 + n)/2} + 2Un^2 + UN^2/2 + \Delta N/2. \quad (6)$$

The tunneling of atoms occurs when the energies E_n^G and E_{n-1}^G are equal to each other. In this situation, a single atom tunnels through the other well. It is analogous to the resonant tunneling in quantum dots due to the Coulomb blockade [25]. By setting $E_n^G = E_{n-1}^G$ in Eq. (6), the tunneling condition for the coupling strength Ω_n can be obtained as

$$\Omega_n = \frac{1}{2} \{ [4U(2n-1) + \Delta]^2 - \Delta^2 \}^{\frac{1}{2}}. \quad (7)$$

In Fig. 3, the values of Ω_n are marked with the red empty circles. This shows that the tunneling condition in Eq. (7) agrees with the exact numerical solution.

IV. ADIABATIC TRANSPORT

We have studied the ground-state properties of the coupled atom-laser system in the previous section. We have shown that the directions of atomic currents and the population difference depend on the coupling strength Ω . Now we study the adiabatic transport of atoms by slowly increasing the coupling strength Ω . According to the adiabatic theorem [26], the system can evolve as its instantaneous ground state if the changing rate of the parameter Ω is sufficiently slow. Therefore, this method can be used for adiabatically transferring the atoms to the other potential well.

We consider the coupling strength $\Omega(t)$ as a linear function of time t , i.e.,

$$\Omega(t) = vt, \quad (8)$$

where v is a positive number. Here the detuning Δ is kept as a constant during the time evolution. Initially, the

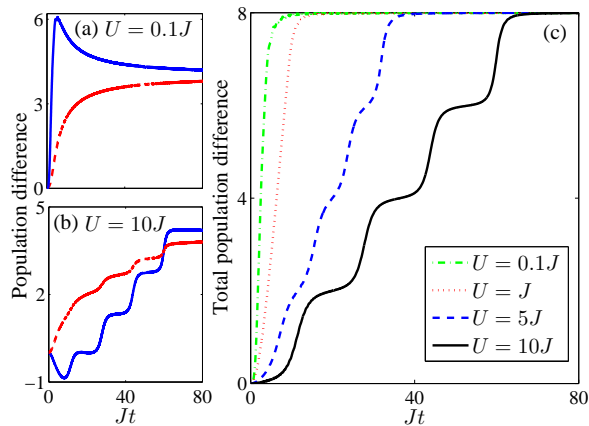


FIG. 4. (Color online) The population differences for the two different component condensates are plotted against the time Jt for $U = 0.1J$ and $10J$ in (a) and (b). The atoms in ground and excited states are denoted by blue-solid and red-dashed lines, respectively. (c) Plot of the total population difference versus the time Jt for different strengths of atomic interactions. The parameters are used: $N = 8$, $\Delta = 20J$ and $v = 2.5J$.

system is prepared in its ground state of the Hamiltonian H_0 in Eq. (1) and setting $\Omega = 0$. The coupling strength $\Omega(t)$ in Eq. (8) is adiabatically increased. In Figs. 4(a) and (b), the population differences are plotted versus the time for the atoms in the different internal states. We can see that the two results in Figs. 2 and 4 reach a good agreement. This shows that the tunneling dynamics of atoms can be controlled by using an external field.

In the regime of weak atomic interactions, the two different component condensates smoothly tunnel through the other well in the same direction in Fig. 4(a). In the opposite interaction limit, the discrete steps are shown in Fig. 4(b). Note that the counter-flow is shown in a short time in figure (b). The flows of atomic spin currents become parallel afterward. This shows that the direction of spin flows can be controlled by appropriately adjusting the parameters Ω and Δ .

Then, we study the time evolution of total population difference of atoms. In Fig. 4(c), we examine the tunneling dynamics for a wide range of interaction parameters. In both regimes, the atoms tunnel to the left potential well when the coupling strength slowly increases with time. The total population differences smoothly increases as a function of time for weak atomic interactions. The discrete steps of the tunneling are shown when the strength of atomic interactions becomes strong. The single-atom tunneling can thus be achieved in the limit of strong atomic interactions.

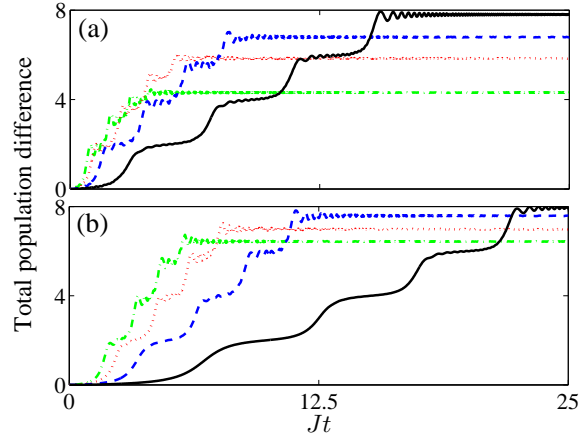


FIG. 5. (Color online) The total population differences are plotted versus the time Jt for the different detunings $\Delta = 20J$ and $200J$ in (a) and (b), respectively. The different rates of change are denoted: $v = 10J$ (black-solid line), $v = 20J$ (blue-dashed line), $v = 30J$ (red-dotted line) and $v = 40J$ (green-dashed-dotted line), respectively. The parameters are used: $N = 8$ and $U = 10J$.

A. Efficiency of the population difference

Next, we investigate the efficiency of the population transfer by increasing the coupling strength of the external field. In Figs. 5(a) and (b), the population differences are plotted versus the time for the two different detunings $\Delta = 20J$ and $200J$. The full population transfer can be achieved if the parameters v are small enough in both cases. When the parameters v become larger, the rates of population transfer increase. However, the smaller population of atoms can be transferred in both cases. It is because they have gone beyond the adiabatic limit. By comparing the figures 5(a) and (b), we find that the larger numbers of atoms can be transported with the same rate v of change for the case using a larger detuning.

B. Effects of the coupling between the laser and the atoms in the neighboring well

Since the separation between the two wells is small [3, 22], the lasers may also couple the atoms in the other potential well. Now we examine a very small coupling between the laser and the atoms in the right potential well. The Hamiltonian, describes the coupling between the laser and the atoms in the right potential well, can be written as

$$H_1^R = \Omega'(e_R^\dagger g_R + g_R^\dagger e_R), \quad (9)$$

where Ω' is the coupling strength between the laser and atoms. Here we consider that the coupling strength Ω' linearly increases with time as

$$\Omega'(t) = v't. \quad (10)$$

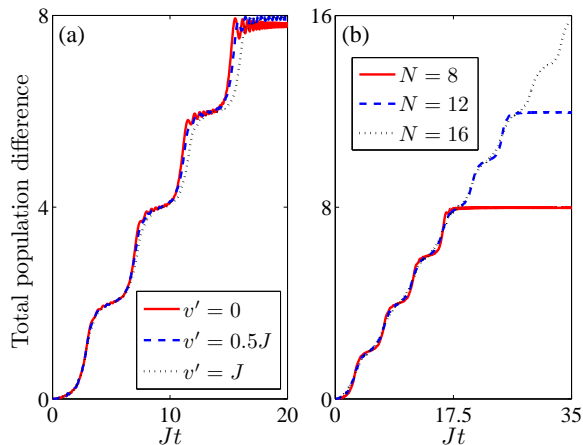


FIG. 6. (Color online) Time evolution of the total population difference. The effect of a small coupling between the laser and the atoms in the right potential well is investigated. In (a), the total population differences are plotted versus the time Jt for different rates of changing v' and $N = 8$. In (b), the total population differences are plotted versus the time Jt for different numbers of atoms and $v' = J$. The parameters are used: $U = 10J$, $\Delta = 20J$ and $v = 10J$.

We assume that the parameter v' is much smaller than v in Eq. (8).

In Fig. 6(a), the total population differences are plotted versus the time for the different rates of changing v' . The atoms can be efficiently transferred from the left to right potential well. The results show slightly different tunneling behaviors for small v' . We then examine the population transfer with small v' for larger number of atoms. In Fig. 6(b), we plot the total population difference as a function of time for different numbers of atoms. The discrete steps of tunneling can be clearly shown. This shows that this method works even if there is a very small coupling between the laser and the atoms in the neighboring well.

V. MULTI-PARTICLE ENTANGLEMENT

Having discussed the tunneling dynamics of atoms, we study the generation of spin-squeezed states by adiabatically changing the coupling strength of the field. To indicate the occurrence of spin squeezing, a parameter ξ^2 can be defined as [17]

$$\xi^2 = \frac{N(\Delta S_{n_1})^2}{\langle S_{n_2} \rangle^2 + \langle S_{n_3} \rangle^2}, \quad (11)$$

where n_i is the i -th component of an angular momentum system, and $i = 1, 2$ and 3 . If ξ is less than one, then the system is said to be spin-squeezed [17]. In addition, the parameter ξ can be used for indicating multi-particle entanglement [18].

Let us define the angular momentum operators as: $S_x = (e_L^\dagger e_R + g_L^\dagger g_R + e_R^\dagger e_L + g_R^\dagger g_L)/2$, $S_y = (e_L^\dagger e_R +$

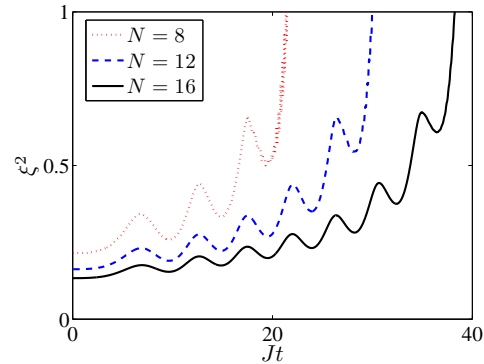


FIG. 7. (Color online) The spin-squeezing parameters ξ^2 are plotted versus the time Jt for different number N of atoms. The parameters are used: $\Delta = 200J$, $U = 10J$ and $v = 10J$.

$g_L^\dagger g_R - e_R^\dagger e_L - g_R^\dagger g_L)/2i$, and $S_z = (e_L^\dagger e_R + g_L^\dagger g_L - e_R^\dagger e_R - g_R^\dagger g_R)/2$. The angular momentum operators obey the standard commutation rule. We study the parameter as

$$\xi^2 = \frac{N(\Delta S_z)^2}{\langle S_x \rangle^2}. \quad (12)$$

Physically speaking, the quantity $(\Delta S_z)^2$ is the variance of the total population difference of atoms between the wells, and $\langle S_x \rangle$ is the sum of the phase coherences between the two wells for the two component condensates.

In Fig. 7, we plot the spin-squeezing parameter ξ^2 versus the time for different number of atoms. Initially, the parameter ξ^2 is below one when $\Omega = 0$. This means that the initial ground state is a spin-squeezed state. As Ω in Eq. (7) slowly increases with time, spin squeezing can be dynamically produced. This result indicates that the system is spin-squeezed for a wide range of Ω . Besides, a higher degree of spin squeezing can be produced with a larger number of atoms N .

VI. CONCLUSIONS

In summary, we have studied how the ground state of a two-component condensate in a double well affected by a local external field. We have shown that the flows of spin currents and particle-tunneling dynamics can be controlled by slowly varying the coupling strength of the external field and appropriately adjusting the detuning. This can be used for studying spin and tunneling phenomena and also the potential applications of atomic devices in atomtronics [27]. In addition, spin-squeezed states can be dynamical generated. It is an important resource for precision measurement [16–18].

ACKNOWLEDGMENTS

This work was partially supported by US National Science Foundation. We would like to also acknowledge the

partial support of National Science Council and NTU-MOE.

Appendix A: Derivation of the effective Hamiltonian for coupling between two internal states and the lasers

The two internal states of an atom can be coupled via pumping to the upper state by two lasers as shown in Fig. 1(b). The Hamiltonian, describes the interaction between the two internal states and the lasers, can be written as

$$H = \omega_{rg}|r\rangle\langle r| + \omega_{eg}|e\rangle\langle e| + \Omega_g[\exp(-i\omega_g t)|r\rangle\langle g| + \text{H.c.}] + \Omega_e[\exp(-i\omega_e t)|r\rangle\langle e| + \text{H.c.}], \quad (\text{A1})$$

By performing the unitary transformation as,

$$U(t) = \exp\{-i[\omega_g|r\rangle\langle r| + (\omega_g + \omega_e)|e\rangle\langle e|]t\}, \quad (\text{A2})$$

the Hamiltonian can be transformed as [24]

$$H' = i\dot{U}^\dagger U + U^\dagger H U, \quad (\text{A3})$$

$$= \Delta_r|r\rangle\langle r| + \Delta_e|e\rangle\langle e| + (\Omega_g|r\rangle\langle g| + \Omega_e|r\rangle\langle e| + \text{H.c.}), \quad (\text{A4})$$

where $\Delta_r = \omega_{rg} - \omega_g$ and $\Delta_e = \omega_{eg} - \omega_g + \omega_e$.

We write the state $|\Psi(t)\rangle$ as,

$$|\Psi(t)\rangle = c_g|g\rangle + c_e|e\rangle + c_r|r\rangle. \quad (\text{A5})$$

From the Schrödinger equation, we can obtain

$$i\dot{c}_g = \Omega_g c_r, \quad (\text{A6})$$

$$i\dot{c}_e = \Delta_e c_e + \Omega_e c_r, \quad (\text{A7})$$

$$i\dot{c}_r = \Delta_r c_r + \Omega_g c_g + \Omega_e c_e. \quad (\text{A8})$$

We assume that Ω_e and Ω_g are real numbers.

If the detuning Δ is much greater than the coupling strengths Ω_e, Ω_g , then the upper state can be adiabatically eliminated. We can obtain

$$c_r \approx -\frac{\Omega_g}{\Delta_r} c_g - \frac{\Omega_e}{\Delta_r} c_e. \quad (\text{A9})$$

The effective Hamiltonian can thus be obtained as

$$H_{\text{eff}} = -\frac{\Omega_g^2}{\Delta_r}|g\rangle\langle g| + \left(\Delta_e - \frac{\Omega_e^2}{\Delta_r}\right)|e\rangle\langle e| + \Omega(|g\rangle\langle e| + \text{H.c.}), \quad (\text{A10})$$

where $\Omega = -\Omega_e \Omega_g / \Delta_r$ is the effective coupling strength between the two internal states $|g\rangle$ and $|e\rangle$. We assume that Ω_g and Ω_e are approximately equal and let $\Delta_e = \Delta$ in Eq. (2).

-
- [1] A. Fert, *Rev. Mod. Phys.* **80**, 1517 (2008).
[2] M. A. Nielsen and I. L. Chuang, *Quantum Computation and Quantum Information* (Cambridge University Press, Cambridge, 2000).
[3] M. Albiez, *et al.*, *Phys. Rev. Lett.* **95**, 010402 (2005).
[4] S. Fölling, *et al.*, *Nature* **448**, 1029 (2007).
[5] W. S. Bakr *et al.*, *Nature* **462** 74 (2009)
[6] C. Weitenberg *et al.*, *Nature* **471**, 319 (2011).
[7] J. Volz *et al.*, *Nature* **475**, 210 (2011).
[8] H. T. Ng, C. K. Law, and P. T. Leung, *Phys. Rev. A* **68**, 013604 (2003).
[9] M. Holthaus, *Phys. Rev. A*, **64**, 011601(R) (2001); C. Weiss and T. Jinasundera, *Phys. Rev. A* **72**, 053626 (2005); T. Jinasundera, C. Weiss, M. Holthaus, *Chem. Phys.* **322**, 118 (2006).
[10] L. Morales-Molina and J. Gong, *Phys. Rev. A* **78**, 041403(R) (2008).
[11] L. Forster, *et al.*, *Phys. Rev. Lett.* **103**, 233001 (2009); Q. Beaufils *et al.*, *ibid.* **106**, 213002 (2011).
[12] D. R. Dounas-Frazer, A. M. Hermundstad and L. D. Carr, *Phys. Rev. Lett.* **99** 200402 (2007); P. Cheinet *et al.*, *ibid.* **101**, 090404 (2008).
[13] C. E. Creffield, *Phys. Rev. Lett.* **99**, 110501 (2007); O. Romero-Isart and J. J. García-Ripoll, *Phys. Rev. A* **76**, 052304 (2007); Y. Qian, Ming Gong and C. Zhang, *ibid.* **84**, 013608 (2011).
[14] D. M. Harber *et al.*, *Phys. Rev. A* **66**, 053616 (2002).
[15] A. B. Kuklov and B. V. Svistunov, *Phys. Rev. Lett.* **90**, 100401 (2003).
[16] M. Kitagawa and M. Ueda, *Phys. Rev. A* **47**, 5138 (1993).
[17] D. J. Wineland, J. J. Bollinger, W. M. Itano and D. J. Heinzen, *Phys. Rev. A* **50**, 67 (1994).
[18] A. Sorensen, L.-M. Duan, I. Cirac, P. Zoller, *Nature* **409**, 63 (2001).
[19] J. Estève *et al.*, *Nature* **455**, 1216 (2008); M. F. Riedel *et al.*, *ibid.* **464**, 1170 (2010).
[20] M. R. Matthews *et al.*, *Phys. Rev. Lett.* **81**, 243 (1998).
[21] G. J. Milburn, J. Corney, E. M. Wright and D. F. Walls, *Phys. Rev. A* **55**, 4318 (1997).
[22] K. Maussang *et al.*, arXiv:1005.1922..
[23] D. A. Steck, Rubidium 87 D line data, <http://steck.us/alkalidata/> (2010)
[24] S. M. Barnett and P. M. Radmore, *Methods in Theoretical Quantum Optics* (Oxford University Press, Oxford, 2002).
[25] C. W. J. Beenakker, *Phys. Rev. B* **44**, 1646 (1991).
[26] A. Messiah, *Quantum Mechanics* (Dover, New York, 1999).
[27] R. A. Pepino, J. Cooper, D. Z. Anderson and M. J. Holland, *Phys. Rev. Lett.* **103**, 140405 (2009).